CHAPTER 189

SAND TRANSPORT RATE UNDER WAVE-CURRENT ACTION

Akira Watanabe¹ and Masahiko Isobe²

Abstract

Laboratory experiments were conducted to obtain data on sand transport processes and transport rates under combined action of waves and currents using an oscillatory-steady flow tank. The sand transport processes were classified into seven types. Four kinds of non-dimensional flow power parameters were defined, and their linear relations with the non-dimensional net transport rates were found for all the transport types.

1. Introduction

Considerable efforts have been devoted in recent years to developing mathematical models of beach evolution, which will be generally classified into three groups: "shoreline change models (e.g. Hanson et al., 1989)", "beach profile change models (e.g. Larson et al., 1989; Watanabe & Dibajnia, 1989), and "beach topography change models (e.g. Watanabe et al., 1986; Vriend & Ribberink, 1989)". Topography change models generally require formulas for estimating local sediment transport rates under combined action of waves and currents. The model developed by Watanabe et al. (1986) employs simple but useful sediment transport formulas based on the power (or energetics) model concept, and has been applied to various engineering practice in Japan (e.g. Shimizu et al., 1990). However we have not yet established highly-reliable formulas to be built in topography change models for accurately evaluating net rates of sediment transport under general conditions of waves and currents.

Purposes of the present study are to obtain fundamental experimental data on net rates of sand transport due to combined action of waves (oscillatory flow) and currents (steady flow) under a simplified condition where the directions of oscillatory and steady flows are parallel, and to investigate relations between the

¹ Professor, Dept. of Civil Eng., Univ. of Tokyo, Bunkyo-ku, Tokyo, 113 Japan.

² Associate Professor, ditto.

net transport rates and relevant hydraulic parameters on the basis of the power model concept.

2. Experimental Procedure and Results

2.1 Experimental procedure

The experiments were conducted using an oscillatory-steady flow tank, in which a steady flow was superimposed in parallel on an oscillatory flow with an arbitrary time variation of velocity as shown in Fig. 1. The time histories of the oscillatory flow velocity were sinusoidal in some cases, but in most case they were non-sinusoidal and asymmetric between positive and negative velocities as illustrated in the figure. The test section was 2 m in length, 24 cm in width and 31 cm in height.

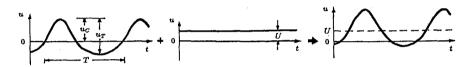


Fig. 1 Definition sketch for combined-oscillatory-steady flow.

The oscillatory flow conditions were changed for the period, T = 3 and 6s, the total amplitude of velocity u_T from 54 to 86 cm/s, and the velocity asymmetry defined by the ratio of the positive (or onshore) velocity amplitude u_C to the total amplitude u_T , for $u_C/u_T = 0.5$ (sinusoidal oscillation), and for 0.6 and 0.7. The steady flow velocity U was also changed between -30 cm/s and +25 cm/s.

Two kinds of sand with the median diameter D = 0.18 and 0.87 mm were used. For each condition, 1) first the sand bed was made even, 2) next oscillatorysteady flow was generated for a time duration of 600T, 3) then bottom profiles in dynamical equilibrium were measured, 4) again the same flow was generated for a period of 10 to 60s, and 5) lastly final bed profiles and volumes of the sand trapped at both ends of the test section were measured. Bed profiles were measured along ten cross-shore lines with electric resistance-type bed profilers. Net rate of sand transport was evaluated at the mid-cross-section of the test section from the bed profile changes and trapped sand volumes.

Sand ripples were formed in all the cases; two-dimensional ripples with long parallel crests in relatively weak flows and three-dimensional ripples with laddershaped short crests in intensive flows. The sand movement was recorded on a VTR. For all the flow conditions, the velocity was measured with an LDV above a fixed flat bed. The velocities measured at an elevation 10 cm above the bed will be used in the following data analysis.

2.2 Net transport rate and sand movement types

Let us define a non-dimensional net sand transport rate Φ by

$$\Phi = \frac{(1 - \epsilon_v) q_{\text{net}}}{w_0 D} \tag{1}$$

where q_{net} is the volumetric net transport rate per unit width per unit time, and ϵ_v , w_0 and D are the porosity, fall velocity and median diameter of the sand, respectively. For the fine sand (D = 0.18 mm), $\epsilon_v = 0.44$ and $w_0 = 2.1 \text{ cm/s}$, whereas for the coarse sand (D = 0.87 mm), $\epsilon_v = 0.47$ and $w_0 = 8.2 \text{ cm/s}$. The direction of the net transport is taken positively into that of the positive (onshore) velocity.

Figure 2 shows the relations between the non-dimensional transport rate Φ and the steady flow velocity U for each oscillatory flow condition for the fine sand. It is seen that the net transport rates are mostly negative, which corresponds to the offshore transport. For example, for the oscillatory flow condition indicated by the inverted triangle symbols, the net transport rates took the largest negative magnitude when there was no steady flow, decreasing in magnitude with the increase in the steady flow velocity U, either positive or negative, and it became positive only for the large positive U.

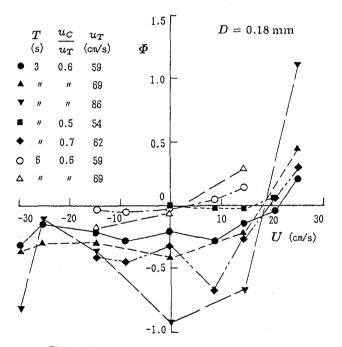


Fig. 2 Non-dimensional net transport rate Φ us. steady flow velocity U for fine sand.

The relations between Φ and U for the coarse sand are shown in Figure 3. For the coarse sand, the net transport rates Φ are mostly positive, namely the onshore transport was predominant even for the negative steady flow velocity U with moderate magnitude.

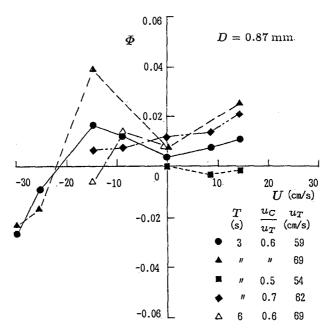


Fig. 3 Non-dimensional net transport rate Φ vs. steady flow velocity U for coarse sand.

These figures indicate that the dependency of the net transport rate on the steady flow velocity and on the oscillatory flow conditions is not simple or monotonic at all. Their interrelations appear too complicated to express by a single general formula.

Now, according to the observation of sand movement in the experiments, it has been concluded that the sand transport processes in the present experiments will be classified into the following seven types.

The first four types are for the fine sand. The sand transport process of **Type I** was observed when T = 3 s and |U| < 20 cm/s. For this type, the sand was set in suspension by lee-vortices formed during positive velocity, and was transported into the offshore direction during negative velocity, whereas the sand suspended during negative velocity was transported shoreward during positive velocity. Because of the asymmetric velocity change, the net transport was into the offshore (negative) direction (see Fig. 4). **Type II** appeared for the cases of

SAND TRANSPORT RATE

strong onshore steady flow (T = 3 s, U > 20 cm/s), and **Type III** took place for those of strong offshore flow (T = 3 s, U < 20 cm/s). For Type II, the sand suspended during the large onshore flow velocity was transported into the shoreward direction (Fig. 5), whereas for Type III, the suspended sand was transported into the offshore direction (Fig. 6). **Type IV** was observed when T = 6 s, namely, the oscillatory flow was of relatively long period. For this type, the sand was suspended up to an elevation higher than in the previous types, and was transported mainly by the steady flow. Hence the direction of the net transport agreed with that of the steady flow (Fig. 7).

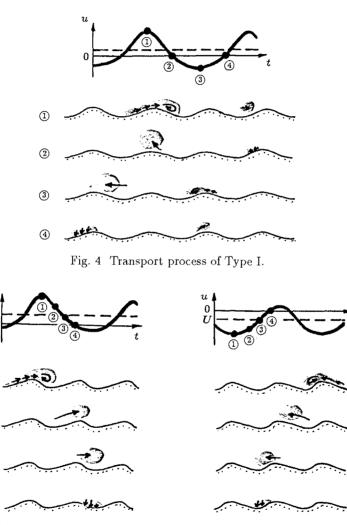


Fig. 5 Transport process of Type II.

(3)

(4)

Fig. 6 Transport process of Type III.

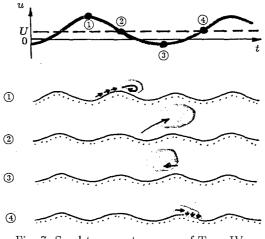


Fig. 7 Sand transport process of Type IV.

The remaining three types are for the coarse sand. **Type V** occurred when $U \ge 0$. For this type, bedload transport was predominant, and the sand was transported into the onshore direction by both the oscillatory flow and the steady flow (Fig. 8). **Type VI** took place when the steady flow was strong and in the off-shore direction (U < -20 cm/s). Again bedload transport was predominant, and the sand was transported into the offshore direction by the very strong offshore flow (Fig. 9). The last type, **Type VII**, appeared when -20 cm/s < U < 0. For this type, the sand suspended during negative velocity as well as bedload during positive velocity contributed to the onshore net transport (Fig. 10).

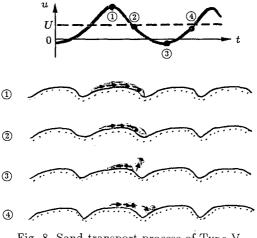


Fig. 8 Sand transport process of Type V.

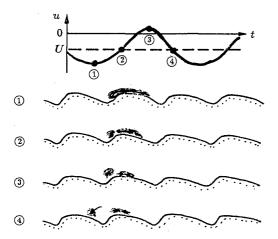


Fig. 9 Sand transport process of Type VI.

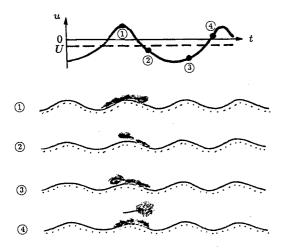


Fig. 10 Sand transport process of Type VII.

3. Net Transport Rate and Flow Power

We will now attempt to relate the net transport rate with the flow condition for each type applying the power model concept. For this let us first define the excursion lengths d_{0+} and d_{0-} and the Shields numbers Ψ_+ and Ψ_- for the positive velocity period T_+ and the negative velocity period T_- , respectively, (see Fig. 11) by

$$d_{0+} = \int_{T_+} u \, dt, \quad d_{0-} = -\int_{T_-} u \, dt \tag{2}$$

$$\Psi_{+} = \frac{f_{cw+} u_{C}^{2}}{2sgD}, \quad \Psi_{-} = \frac{f_{cw-} (u_{T} - u_{C})^{2}}{2sgD}$$
(3)

where $s (= \rho_s/\rho - 1)$ is the immersed specific gravity of the sand, and f_{cw+} and f_{cw-} are the friction factors in a coexistent wave-current field and are determined from the hypothetical sinusoidal oscillation velocities and the steady flow velocity (Fig. 11) with the frictional law proposed by Tanaka and Shuto (1981). The median diameter D of the sand grains was used as the equivalent roughness $k_s (= 30z_0)$ in spite of the presence of sand ripples.

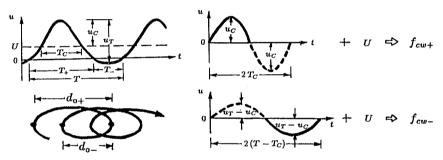


Fig. 11 Definition sketch for computing excursion lengths and Shields numbers.

With the consideration of the transport processes for the above seven types, let us further define four kinds of non-dimensional flow powers, P_1 , P_{11} , P_{111} and P_{1V} , and examine their correlations with the non-dimensional transport rate Φ .

a) Type I

On the basis of the power model concept, we assume that the immersedweight of the sand set in suspension per unit horizontal area during the positive velocity period T_+ is proportional to the excess shear stress $(\tau_+ - \tau_C)$ times (T_+/T) , where $\tau_+ = \rho sg D\Psi_+$ is the amplitude of the bed shear stress during T_+ , and τ_C the critical shear stress for the onset of the general movement. We further assume that the offshore displacement of this suspended sand during $T_$ is proportional to the excursion length d_{0-} . Then the resultant offshore transport rate q_- averaged over the period T is to be proportional to a kind of flow power $(\tau_+ - \tau_C) (T_+/T) (d_{0-}/T)$. In a similar way, the onshore transport rate q_+ will be in proportion to $(\tau_- - \tau_C) (T_-/T) (d_{0+}/T)$, and then the net transport rate q_{net} will be given by the difference between q_+ and q_- . Hence if we define a non-dimensional flow power P_{I} by

$$P_{\rm I} = (\Psi_{-} - \Psi_{C}) \frac{T_{-}}{T} \frac{d_{0+}}{w_{0}T} - (\Psi_{+} - \Psi_{C}) \frac{T_{+}}{T} \frac{d_{0-}}{w_{0}T}$$
(4)

where Ψ_C is the critical Shields number, then we can expect the non-dimensional net transport rate Φ to be proportional to $P_{\rm I}$.

Figure 12 shows the relation between Φ and $P_{\rm I}$ for Type I. Since this type includes the transport of the fine sand only, the critical Shields number Ψ_C was set as equal to 0.11 (see Watanabe et al., 1981). Although the scatter of the plotted data is not small, it is clear that Φ and $P_{\rm I}$ have a positive correlation, which is expressed approximately by the following linear relation:

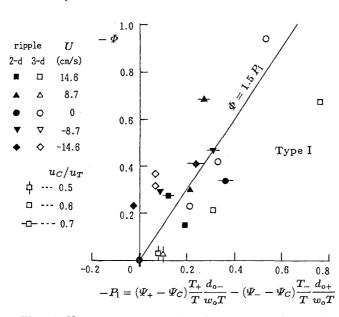


Fig. 12 Net transport rate Φ vs. flow power $P_{\rm I}$ (Type I).

b) Types II, III, V and VI

 $\Phi = 1.5 P_{\rm I}$

In the transport processes of these four types, just contrary to Type I, the sand set in motion by the onshore flow was transported into the onshore direction, and the one agitated by the offshore flow was carried toward the offshore. Hence we define a non-dimensional flow power $P_{\rm II}$ by

$$P_{\rm II} = (\Psi_+ - \Psi_C) \frac{T_+}{T} \frac{d_{0+}}{w_0 T} - (\Psi_- - \Psi_C) \frac{T_-}{T} \frac{d_{0-}}{w_0 T}$$
(6)

According to Watanabe et al. (1981), a value of Ψ_C for the coarse sand (Types V and VI) should be about 0.06, but it was changed to 0.04, because noticeable sand movement was observed even when $\Psi_C < 0.06$ in the experiments.

(5)

The results shown in Fig. 13 indicate that, although the data for Type II show much scatter and are deviated from those for the other types, an overall relation is expressed fairly well by

 $\Phi = 0.15 P_{\rm H}$



(7)

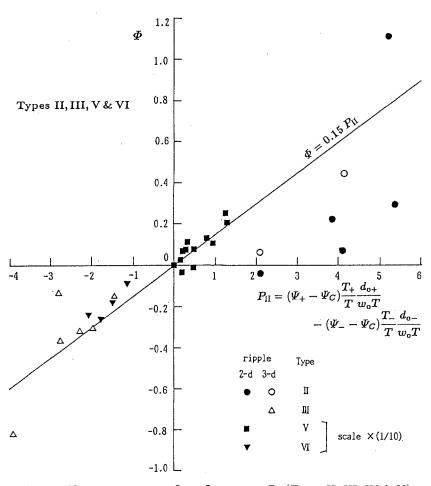


Fig. 13 Net transport rate Φ vs. flow power P_{II} (Types II, III, IV & V).

c) Type VII

For this type, both the bedload during the positive velocity period and the sand suspended during the negative velocity period contributed to the onshore net transport. Therefore the combination of the onshore components of $P_{\rm I}$ and $P_{\rm II}$ will be appropriate as an effective flow power $P_{\rm III}$ for Type VII, which is defined by

$$P_{\rm III} = (\Psi_{-} - \Psi_{C}) \frac{T_{-}}{T} \frac{d_{0+}}{w_{0}T} + 0.1 \left(\Psi_{+} - \Psi_{C}\right) \frac{T_{+}}{T} \frac{d_{0+}}{w_{0}T}$$
(8)

where the factor of 0.1 in the second term was determined by considering the proportionality coefficients in Eqs. 5 and 7.

Figure 14 shows the relation of Φ with $P_{\rm HI}$, which is well approximated by $\Phi = 2.7 P_{\rm HI}$ (9)

It should be noted that the sand ripples were two-dimensional in all the cases of this type.

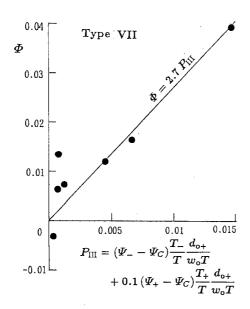


Fig. 14 Net transport rate Φ vs. flow power P_{III} (Type VII).

d) Type IV

For this type, the suspended sand was transported mainly by the steady flow, and the direction of the net transport changed with that of the steady flow. (The sand ripples were three-dimensional.) Hence the net transport rate will be given by the summation of the component due to the steady flow and that due to the oscillatory flow as in the transport rate formula proposed by Watanabe et al. (1986). Let us therefore define a non-dimensional flow power P_{1V} for this type by

$$P_{\rm IV} = (\bar{\Psi}_C - \Psi_C) \frac{6U - u_T/2}{w_0}$$
(10)

where $\overline{\Psi}_C$ is the representative time-mean Shields number defined by

$$\overline{\Psi}_C = \frac{\Psi_+ T_+ + \Psi_- T_-}{T} \tag{11}$$

The relation between Φ and $P_{\rm IV}$ for this type is shown in Fig. 15, and is approximately expressed by

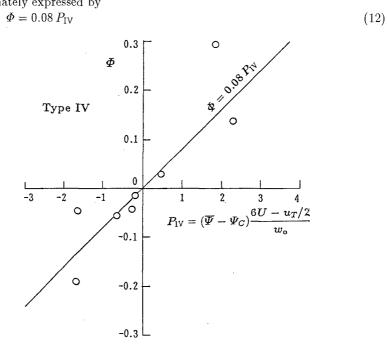


Fig. 15 Net transport rate Φ vs. flow power P_{IV} (Type IV).

4. Concluding Remarks

Experimental data were obtained on the net sand transport rate in combinedparallel-oscillatory-steady flows. The sand transport processes in the experiments were classified into seven types. Considering typical features of the transport process of each type, we defined four kinds of non-dimensional flow power, and found that the net transport rates under combined action of waves (oscillatory flow) and currents (steady flow) were well correlated to the relevant flow powers. It should be mentioned that the relations between the non-dimensional net transport rates and flow powers obtained in this study don't involve explicitly the size and shape of sand ripples in spite of their presence.

The formulas presented in this paper cannot be directly built in mathematical models; we need to accumulate more experimental data and to study more detailed sand transport processes. However these results would provide us yet with very useful information such as for the establishment of generalized sediment transport rate formulas, and for the development of numerical simulation models of sand grain motion over a rippled bed under waves and currents, on which our group is now working. This paper is a part of the outcomes of our study supported by National Science Foundation of the Ministry of Education, Science and Culture, to which we would like to express our thanks. We also appreciate the efforts of Mr. M. Sakinada in conducting the experiments.

REFERENCES

Hanson, H., M. B. Gravens and N. C. Kraus (1989): Prototype applications of a generalized shoreline change numerical model, *Proc. 21st ICCE*, ASCE, pp. 1265-1279.

Larson, M., N.C. Kraus and T. Sunamura (1989): Beach profile change: morphology, transport rate and numerical simulation, *Proc. 21st ICCE*, ASCE, pp. 1295-1309.

Shimizu, T., H. Nodani and K. Kondo (1990): Practical application of the three-dimensional beach evolution model, *Abstracts*, 22nd ICCE, pp. 407-408.

Tanaka, H. and N. Shuto (1981): Friction coefficient for a wave-current coexistent system, *Coastal Eng. in Japan*, JSCE, Vol. 24, pp. 105-128.

Vriend, H. J. de and J. S. Ribberink (1989): A quasi-3D mathematical model of coastal morphology, *Proc. 21st ICCE*, ASCE, pp. 1689-1703.

Watanabe, A., Y. Riho and K. Horikawa (1981): Beach profile and onoffshore sediment transport, *Proc. 17th ICCE*, ASCE, pp. 1106-1121.

Watanabe, A., K. Maruyama, T. Shimizu and T. Sakakiyama (1986): Numerical prediction model of three-dimensional beach deformation around a structure, *Coastal Eng. in Japan*, JSCE, Vol. 29, pp. 179-194.

Watanabe, A. and M. Dibajnia (1989): Numerical modeling of nearshore waves, cross-shore sediment transport and beach profile change, *Proc. IAHR Symp. on Mathematical Modelling of Sediment Transport In the Coastal Zone*, pp. 166-174.